Kirkendall effect in liquid during the *in situ* processing of metal matrix composites under micro-gravity conditions

L. ANESTIEV, L. FROYEN, L. VAN VUGT
KULeuven, Kasteelpark Arenberg 44, B-3001 Heverlee, Belgium
E-mail: ludo.froyen@mtm.kuleuven.ac.bc

Some interesting and unexpected effects observed during the *in situ* production of an Al-TiB$_2$ metal matrix composite during the STS95, SPACE-SHUTTLE (1998) mission are described. It is shown that during the processing of the composites a Kirkendall effect in the liquid is observed. In contrast with the classical effect, this is due not only to the considerable diffusivity difference between the B and Ti in the Al matrix, but also to the chemical reaction taking place to form TiB$_2$. © *2002 Kluwer Academic Publishers*

1. Introduction

Metal matrix composites have many desirable characteristics for precision components: e.g. light weight, dimensional stability and high thermal conductivity [1, 2]. They offer the stiffness of iron at about one third of the weight and are therefore attractive for application in the automotive and aerospace industries. The main advantages of liquid processing are the low cost, the almost unlimited freedom of design and suitability for continuous processing. One of the successful metal matrix composites is Al/TiB$_2$, which is based on the super-hard TiB$_2$ reinforcement and an aluminium matrix, where properties such as ductility are combined with the strength and hardness provided by the TiB$_2$.

To study the reactive synthesis of TiB$_2$ in an Al-matrix, the following model experiment is conceived. Two pieces of Al-Ti and Al-B alloy are connected and melted. Due to the diffusion of the dissolved components, in this case Ti and B, a reaction starts, leading to the formation of the desired reinforcement phase TiB$_2$. Unfortunately because of the considerable difference between the specific weights of the reinforcement particles and the Al matrix sedimentation occurs, which leads to the non-uniform distribution of the TiB$_2$ particles in the matrix. Fig. 1 shows a typical result from the specimens processed under earth conditions. Note the specific deformation of the reaction zone which is characteristic to all processed specimens. The explanation of the so obtained results has been ascribed to the liquid metal flow induced by the movement of the TiB$_2$ particles. Indeed, because the buoyancy force is smaller than the gravitational force, a movement of the formed particles should occur in the direction of the gravity force. According to the Stokes-Einstein equation, the friction between the TiB$_2$ particles and the liquid will lead to a buoyancy-driven flow inside the liquid. This flow can be considered as laminar, because of the low value of the induced velocities. It is understandable that the flow pattern across the cross-section of the crucible

is not constant. Due to the friction between the crucible walls and the moving liquid the liquid, at the center of the crucible should flow faster than that near the walls. This flow pattern is known as Poiseuille flow and is typical for the flow of viscous liquid between restricting planes or geometrically shaped walls. As seen from Fig. 1 this is actually the observed case. The flow of the central section is faster than the ones close to the crucible walls. Unfortunately, the literature on the description of the processes occurring during the *in situ* forming of metal matrix composites is still very scarce. So, it is not possible to compare these results and explanations with those of other authors. Since the initial aim was to study the influence of temperature and diffusion on the precipitation rate and the distribution of the TiB$_2$ particles along the specimen, the influence of gravity should be removed. Thus, a micro-gravity experiment was planned and carried out in the STS95 mission of the SPACE SHUTTLE (1998).

2. Experimental details

Four samples were processed and analyzed. Each sample consisted of two pieces of equal length (10 mm) and diameter (8 mm), Al-B and Al-Ti alloys connected by friction welding. Two samples were made from Al alloys with 1 at.% B and 0.5 at.% Ti, and the other two from Al alloys with 2 at.% B and 1 at.% Ti. Before starting the micro-gravity experiments the samples were heated to 400°C for 4 hours in air to form a protective layer in order to avoid Marangoni convection during the space experiments. The so prepared samples were heated up to, 800 and 900 (the samples with composition Al-B$_{1\,at.\%}$-Ti$_{0.5\,at.\%}$) and to 1000, and 1100°C (the samples with composition Al-B$_{2\,at.\%}$-Ti$_{1at.\%}$) in Ar atmosphere and kept at that temperature for about 30 min. under micro-gravity conditions, during the STS-95 mission. Thus, the dissolved Ti and B diffused into the opposite parts of the specimen and reacted with each
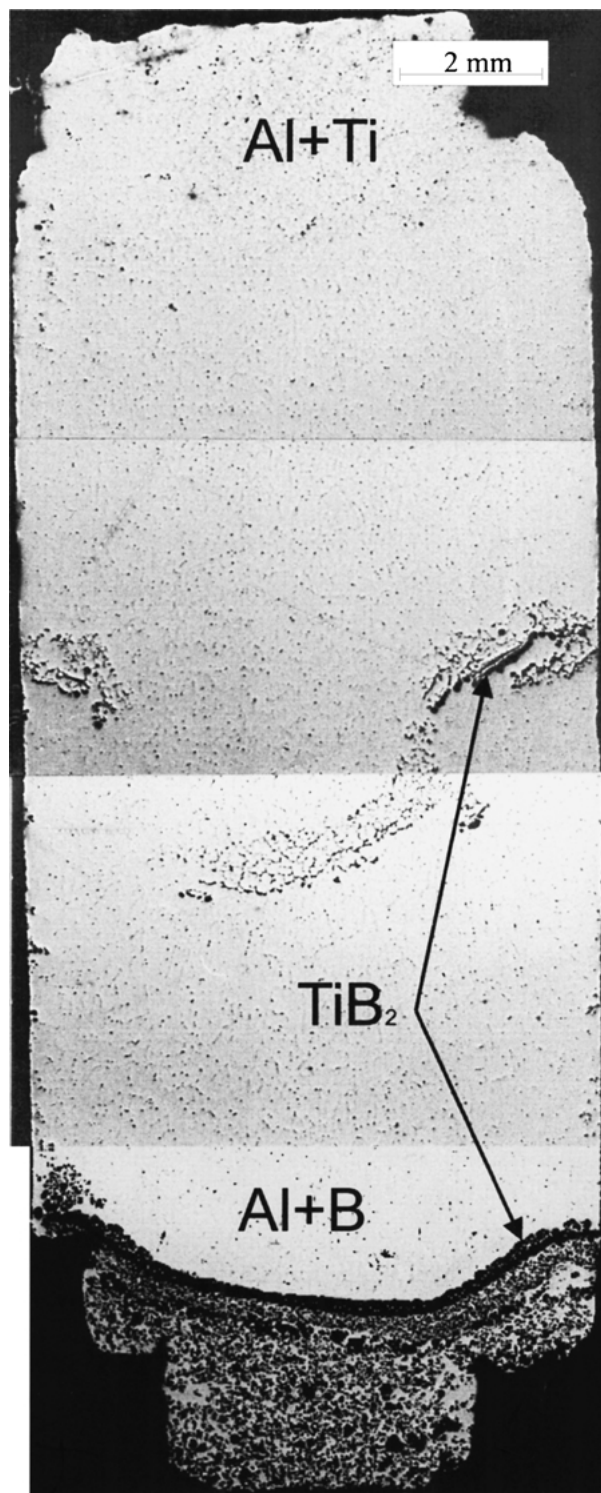
Figure 1 Micrograph of specimen processed under earth conditions. Note the sedimented TiB$_2$ particles at the bottom of the crucible and the specific deformation pattern of the reaction zone, which is typical of all specimens processed.

other to form TiB$_2$. During the micro-gravity experiments special care was taken to avoid any action inducing gravity-like effects. All the experiments were carried out during the sleeping time of the astronauts. Special care was also taken to have a negligible temperature gradient along the specimens during the experiment. For this purpose a specially constructed multi-zone furnace (see Fig. 2) was used. This consisted of two main zones: a heating zone, in which the experiment was carried out and cooling zone into which the

specimens were pushed to cool down at the end of the experiment. Unfortunately, because of the space limitations imposed by the nature of the experiment, only the first two specimens i.e. these processed at 800° and 900°C were quenched. The other two specimens were cooled down at a considerably lower rate estimated to be about 10–15 K/min.

3. Results

The micrographs in Fig. 3 show typical microstructures of the contact zone of the samples after the experiment. The reaction zone with the formed TiB$_2$ (white) is clearly visible in the middle of every specimen. It is interesting to note that the reaction zone splits into two parts separated by a zone of almost pure Al. This interesting behavior was unexpected. As shown previously [3] this is due to differences in the reaction rates on either side of the contact zone. Another interesting observation is that the characteristic deformation of the reaction zone persisted in the micro-gravity experiments. This rules out Poiseuille flow as the only cause of the reaction zone deformation.

The analysis of the experimental evidence lead to the following results:

1. At 800° and 900°C the reaction zone is deformed on the boron side of the specimen (left part of the micrographs). It should be noted that B is the component with the higher diffusivity in the Al matrix. Unfortunately no data for the diffusion coefficients of boron and titanium in aluminium were found. The ratio between D_B and D_{Ti} in Al is estimated to be about 2 [4].

2. For the experiment at 1000°C, the deformation of the reaction zone is not so pronounced, although a little deformation of the reaction zone is observed on the boron side part of the specimen.

3. For all the temperatures studied a volume deficiency is observed around the contact between the reaction zone and the surface of the specimens. It is interesting to note that these deficiencies occur only on the boron side. There is a very well pronounced deficiency of the specimen processed in 900°C (see Fig. 3b). In this case it extends along the whole boron side of the specimen in contrast to the other studied temperatures. For the 800° and 1000°C specimens the volume deficiency is restricted to around the reaction zone only (see Fig. 3a and c)

4. The existence of pores is a characteristic of all the cases. It should be noted, however that the porosity is more noticeable in the 1000°C specimen. This is probably due to the fact that this specimen has been cooled relatively slowly, which allowed the smaller pores to coagulate into bigger ones (see Fig. 3c). Porosity is found on both sides of the reaction zone, although it is somewhat more pronounced on the Ti-side.

5. In some of the specimens, several reaction zones can be destinguished. The most obvious is the 900°C specimen (see Fig. 3b). At least three reaction zones can be distinguished in this case. The same is found for the 800°C specimen, but the reaction zones are not so easily distinguished from each other.

6. The specimen processed at the highest temperature e.g. 1100°C does not show the patterns observed at
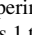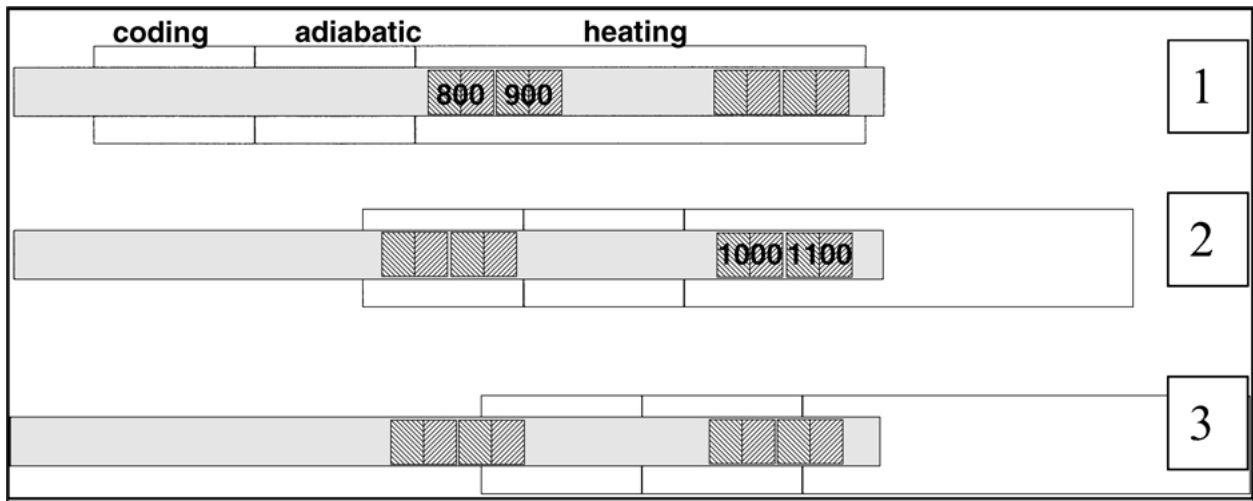
Figure 2 Schematic diagram of the space experiment. ▨▨ represents one sample consisting of Al + B (left) and Al + Ti (right). The temperature, (in °C), is shown on the specimens. The numbers 1 to 3 (on the right side) denote different stages of the experiment.

the lower temperatures. In order to study the processes of metal matrix formation, a theoretical model was developed [3]. The model showed that the concentrations of the dissolved components in the reaction zone for this case are around $X_B = 0.08$ at.% and $X_{Ti} = 0.01$ at.%, with X_B and X_{Ti} as atomic fractions of B and Ti. At this composition, the temperature is close to the liquidus temperature [5, 6]. The model presented in [3] also predicted a broad frequency function of the radii distribution of the precipitates (see Fig. 4 in [3]), which combined with the long processing time gives a favorable condition for an intensive coarsening process. It is very difficult to separate the effects resulting from the interference of the coarsening processes and the process of diffusion precipitation. Therefore, this specimen is excluded from the further discussion.

7. The formation of needlelike crystals of Al₃Ti is observed in the specimen processed at 1000°C (see Fig. 3c). These are formed during the cooling of the specimen. As mentioned above the specimens processed at higher temperatures (1000°C and 1100°C) have been cooled down at relatively lower cooling rates, which give favorable conditions for the formation of needlelike crystals of Al₃Ti during cooling.

8. Fig. 4 shows the specimen processed at 800°C. The initial and final positions of the contact plane, as well as the real specimen dimensions, are indicated on the figure. This specimen is used because it is less deformed due to the surface tension. Therefore, the observed shift is purely due to the Kirkendall effect as discussed below. The maximum shift of the plane Δx_{max} is about 3.5 mm, which compared to the length of the specimen (20 mm), is a considerable change.

4. Discussion

Three possible effects may lead to the formation of the structures observed in Fig. 3a–c, which are independent of the presence or absence of gravity. These are the Marangoni effect [7–9], thermodynamic effects due to the Ti and B dissolving and forming of TiB₂ in the Al-matrix and Kirkendall effect [10–22]. The first of these can be ruled out since special care was

taken during the preparation of the specimens to avoid it. Moreover, the Marangoni effect would not cause the split of the reaction zone and the volume deficiency of the boron side. On the contrary, if there is a Marangoni effect present, this would lead to the mixing of the two aluminium alloys and to a homogeneous distribution of the formed TiB₂ along the specimen. For the same reasons, it is difficult to explain the observed volume deficiency and pore formation.

It is well known that dissolution or precipitation may lead to volume changes due to associative or rejective forces between the molecules of the solvent and the solute. Unfortunately, the partial volumes of the dissolved B and Ti in Al are unknown and thus cannot be
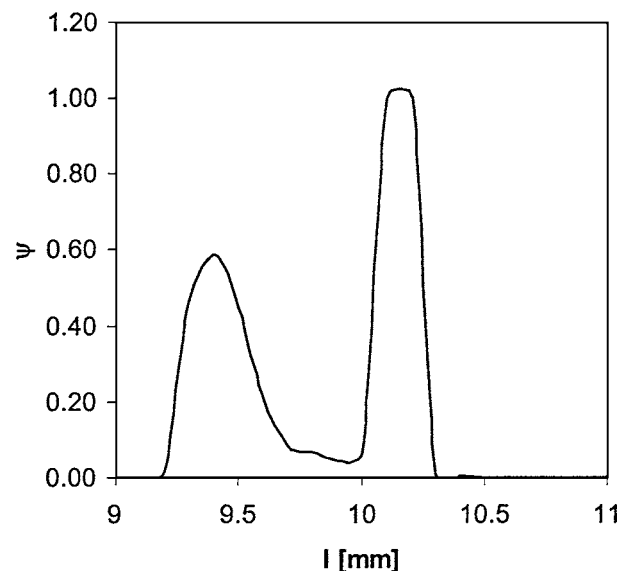

Figure 3 Micrographs of the contact zone of the specimens processed under micro-gravity conditions at temperatures of (a) 800°C, (b) 900°C, (c) 1000°C and (d) 1100°C. The initial parts of the specimen i.e. Al-B and Al-Ti are labeled at the bottom of every micrograph. Note the specific deformation pattern of the reaction zone, typical of all the specimens processed and the characteristic split to give reaction product on both sides of the contact zone. TiB₂ particles (white) and pores (black) are clearly visible in the central sections of the micrographs. The needlelike crystals of TiAl₃ (Fig. 3c) were formed during the cooling of the specimen (*Continued*).

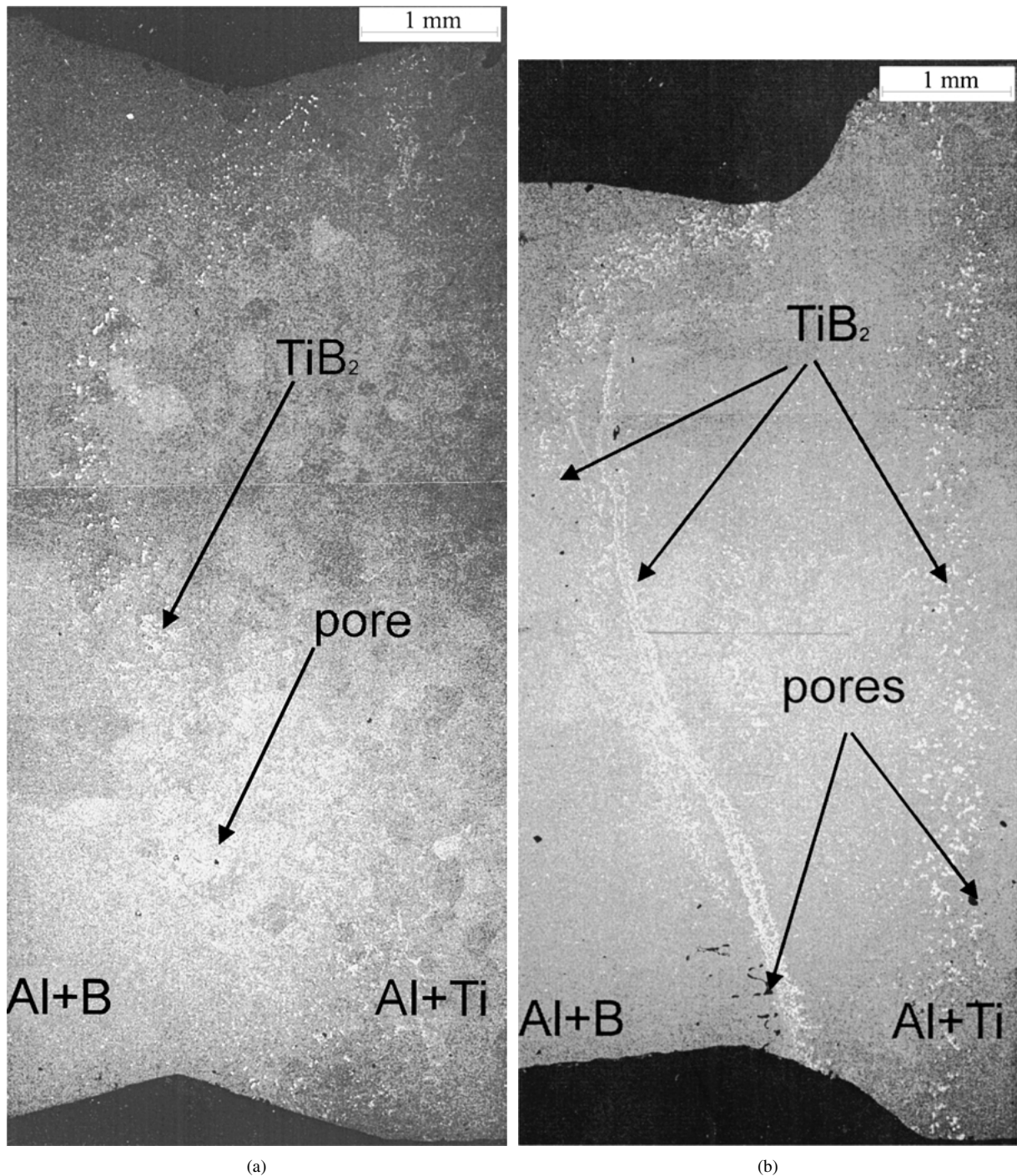(a)   (b)
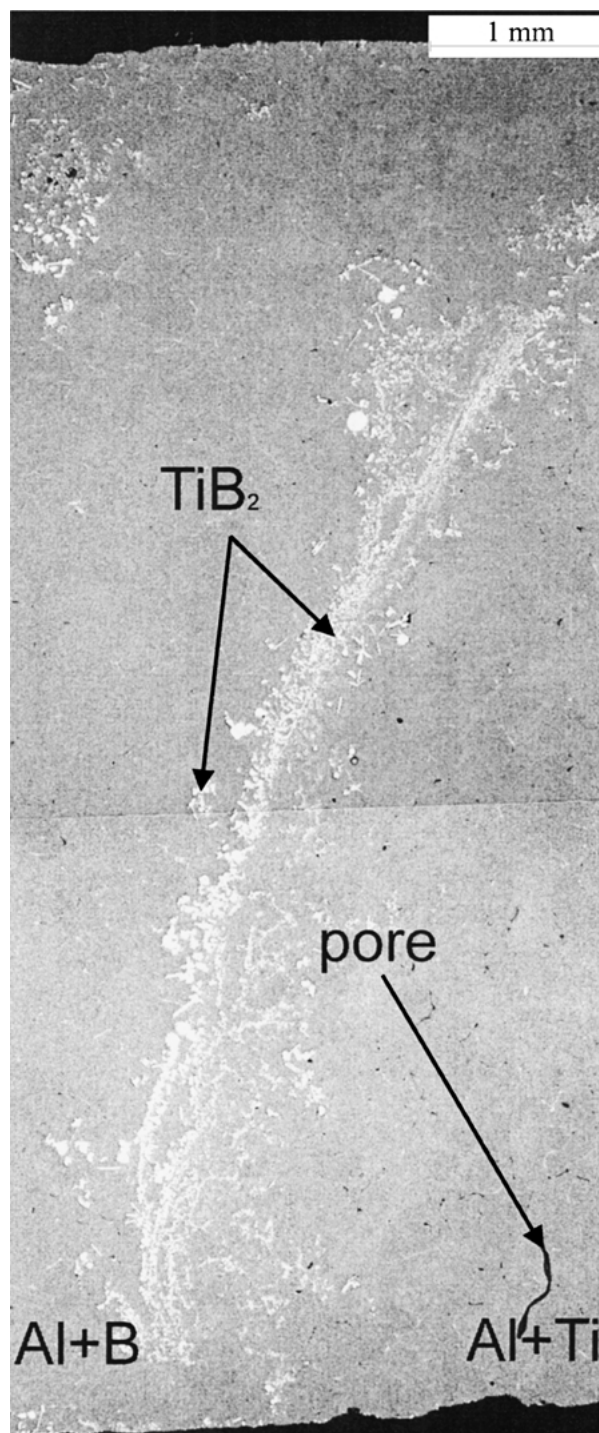
Figure 3 (Continued).

used to investigate the likely magnitude of a thermodynamic effect. However, the observed shift of the contact zone is large. Only a few of the systems, studied up to now, exhibit a considerable volume change during mixing [10]. Therefore, it is unlikely that a thermodynamic effect is responsible for the experimental observations reported here. Thus, the only remaining possibility is that the deformation of the reaction zone occurs due to a Kirkendall shift of the Al-B/Al-Ti contact zone.

The Kirkendall effect [11, 12, 17, 18] was first demonstrated, and is usually observed, when two solid pieces of pure metal (or metal and alloy) with different diffusion coefficients are placed together and annealed for a long time: a shift of the initial contact surface is observed with respect to the end of the couple. The

atoms of the metal with the higher diffusivity penetrate the one with the lower diffusivity at a faster rate. As a result, one of the parts increases its volume in order to accommodate the net positive inward flux of matter. This increase should lead to a shift of the contact interface towards the side of the element with the faster diffusion. If the contact zone is marked with some inert markers, this shift can be visualized. Smigelkas and Kirkendall [11, 12] demonstrated this effect experimentally for the first time on copper-zinc alloys. Zinc is a faster diffuser and the marked zone (called the Kirkendall plane) shifts towards the zinc-reach side of the couple. Although the classical experiment uses solid metals and alloys, this effect should also be observed in liquids, since the first convincing interpretations of
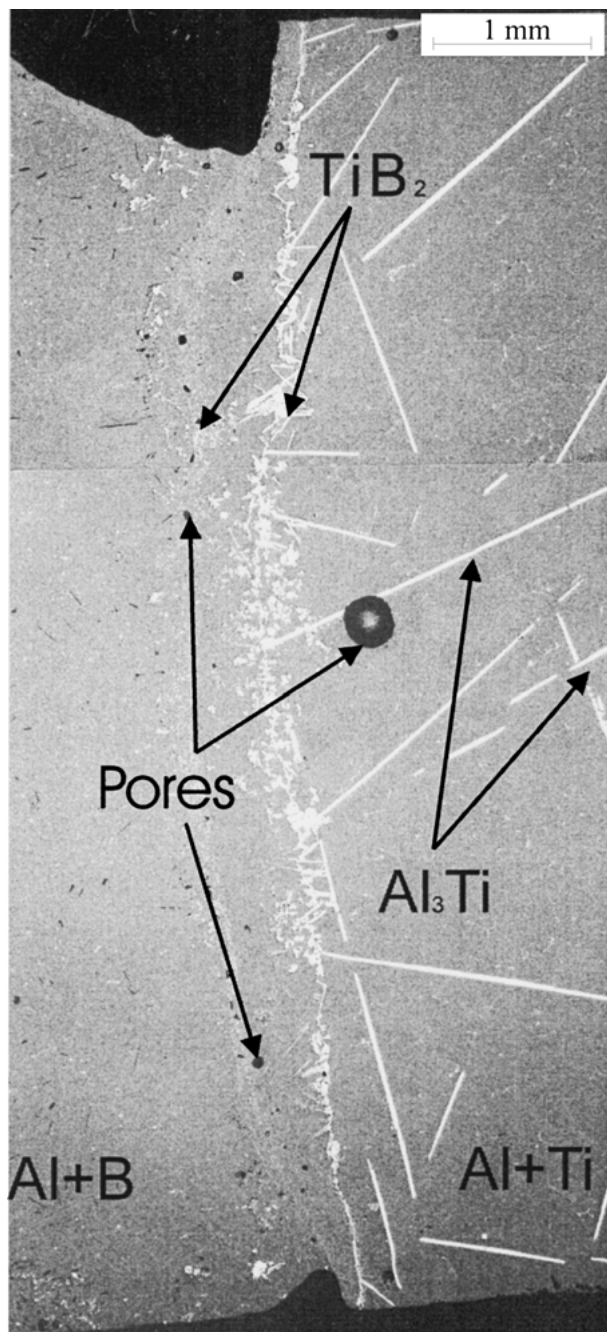
(c)

(d)

Figure 3 (*Continued*).

the phenomenon given by Darken [13] and later extended by Manning [14] is not based on any detailed mechanism for mass transport [17].

The formation of pores is also characteristic of the Kirkendall effect. Indeed, sometimes the flow of the liquid cannot compensate for the excess vacancies formed due to the diffusivity of the faster component. In this case the vacancies may coagulate (condense) and form pores (voids). This phenomenon is known as diffusion porosity [18]. The porosity formation is facilitated when the material contains dissolved gases. As mentioned above, the observed effect was not expected, therefore no special care was taken to reduce the dissolved gases in these specimens. It is worth noting that

the diffusion porosity is usually not observed in carefully annealed specimens.

In the concrete case discussed here, the faster diffuser is the boron, the boron side of the specimen should be in a state of tension and the titanium side should be compressed. Therefore, pores should exist at the boron side of the specimen. Fig. 3 however, shows that this is not the case. Some of the pores formed on the titanium side of the specimen (the upper side of Fig. 3a to c). Thus, the classical explanation of the Kirkendall effect does not work in this case, since the formation of pores at the titanium side cannot be explained. Rather, the formation of TiB_2 in the contact zone causes this effect. Indeed, the reaction zone serves as a sink for both
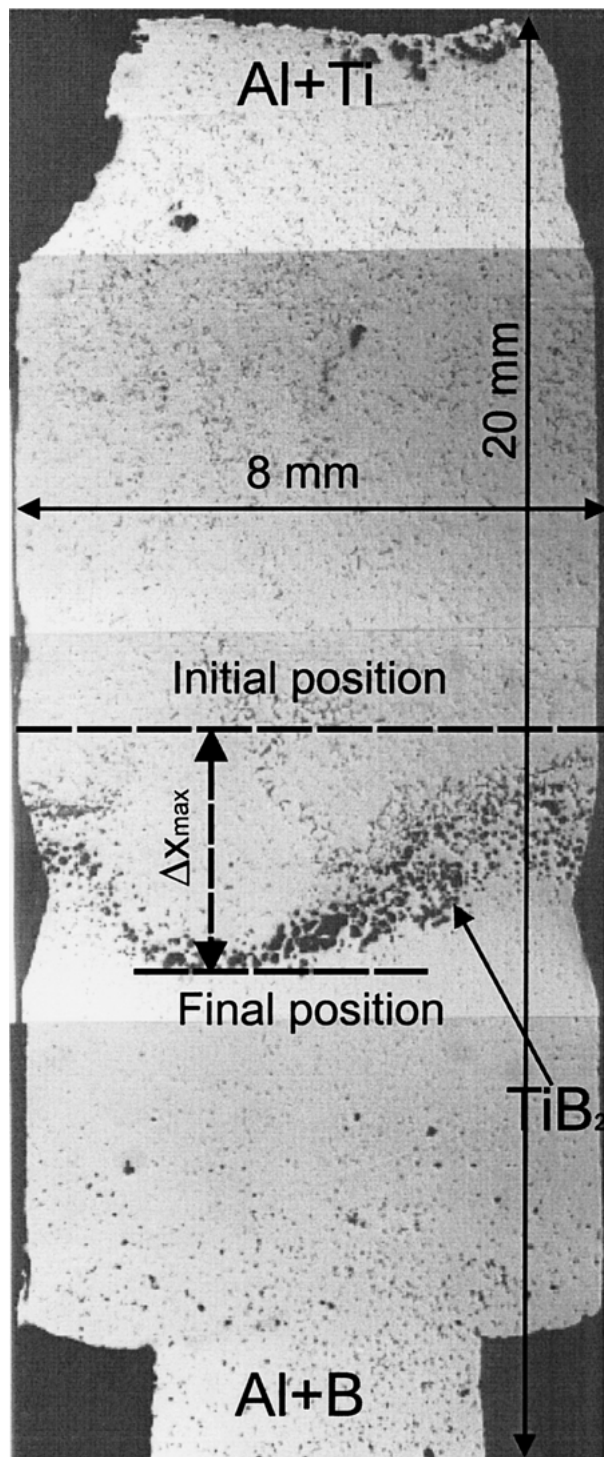
1911

Figure 4 Micrograph of the specimen processed at 800°C. The dimensions (length and width) as well as the initial and the final positions of the contact zone (reaction zone) are shown. The maximum shift of the plane Δx_{max} is about 3.5 mm, which, compared to the specimen length (20 mm), is a considerable change.

the diffusing boron and titanium. Therefore, behind the reaction zone (the Ti side of the specimen) the boron concentration is much lower than when no reaction is occurring. Since there is no considerable diffusion of boron in the titanium part no vacancy deficiency is observed, as in the classical Kirkendall effect. On the contrary, since the reaction zone serves also as a sink for Ti atoms it is also in tension, due to the Ti diffusion into the reaction zone. This leads to the very interesting situation that there is an excess of vacancies on both sides

of the specimen giving pores not only on the boron side but also on the titanium side of the specimen. It also explains why the pores on the titanium side are so close to the reaction zone. The shift of the reaction zone in the direction of the boron side occurs since the boron part, should be more in tension for two reasons. Firstly boron is a faster diffuser than titanium, and secondly to form a molecule of TiB_2 two boron atoms and one titanium atom are required.

The existence of multiple reaction zones in some of the specimens can be explained as follows. The first of the formed reaction zones (the most deformed one) is moved due to a compensation flow towards the boron side i.e. the regions which are poor on titanium. As a result, the precipitation rates of TiB_2 decreases or even stops. Conversely, the diffusion of boron into regions, which are richer in titanium, forms a new reaction zone, which in turn experiences the same shift. As noted in the previous section, this process is repeated at least three times. No such multiple reaction zones were observed in the 1000°C specimen. In this specimen the reaction rate should be higher than for the 800° and 900°C specimens, because of the combined effects of the higher temperature and the higher concentration of the reacting components (2 at.% B and 1 at.% Ti). The fast reaction rate produces a dense layer of TiB_2, which effectively blocks the diffusion of the boron and titanium. Therefore, several seconds after the start of the experiment the reaction actually stops. This is confirmed also by the calculation [3]. This also explains why there is no pronounced deformation of the reaction zone. If diffusion stops, TiB_2 formation and thus the Kirkendall shift stop.

The volume deficiency and the form of the reaction zone are also explained assuming that the observed shift of the reaction zone is due to Kirkendall effect. As pointed out above, in this case the combined action of the high boron diffusivity and the TiB_2 formation induces a vacancy gradient inside the specimens. This vacancy gradient can be compensated for by flow of the liquid metal and from the action of the surface tension. However, due to the internal friction inside the liquid metal (high viscosity of the particle-liquid suspension) the liquid flow can not compensate immediately the arising tension. Therefore, it is partially compensated for by the surface tension giving use to the deformations observed in the reaction zone section of the specimens.

The unequal shift velocity of the reaction zone is similarly explained. As seen from Fig. 3, the central parts of the reaction zone are more deformed than peripheral ones. This is due to the fact that near the wall of the specimen, part of the vacancy excess is compensated for the surface tension. Thus the vacancy gradient which is the driving force of the process is different for different parts of the cross-section. This inequality leads to different velocities for the Kirkendall plane, as observed in Fig. 3a–c.

5. Conclusions
A case of Kirkendall shift in liquid Al + B/Al + Ti specimens has been described. In contrast to the classical Kirkendall effect, the driving force for the shift of the

Kirkendall plane is diffusion coupled with reaction. Since the specimens are in the liquid state and under micro-gravity the influence of the surface tension on the Kirkendall shift is clearly visible. In the explanations of the experimental evidence, it is unambiguously shown that the observed effect is due to Kirkendall shift and not to some other effects which may also take place at micro-gravity.

References
1. A. GEIBEL, L. DELAEY and L. FROYEN, *Scripta Met. and Mater.* **43** (1996) 889.
2. L. FROYEN, in Proceedings of the 8th International Microgravity Summer School, Schnellenberg, June 1994, Germany, p. 49.
3. L. ANESTIEV, L. FROYEN and L. VAN VUGT, *J. Appl. Phys.*, accepted for publication.
4. T. EJIMA and T. YAMAMURA, in Proceedings 2nd Int. Conference "The Properties of Liquid Metals," edited by S. Takeuchi, 3–8 September 1972, Tokyo, Japan, p. 537.
5. F. H. HAYES, H. L. LUKAS, G. EFFENBERG and G. PETZOW, *Z. fuer Metallkde* **80** (1989) 361.
6. J. FJELLSTEDT and A. E. W. JARFORS, in "On the Al-Ti-B phase diagram," IISRN KTH/MG-INR-009-SE, Metals Casting Group, The Royal Institute of Technology, June 1997, Stockholm.
7. Y. MALMEJAC and G. FROHBERG, in "Fluid Science and Materials Science in Space," edited by H. U. Walter (Springer-Verlag, New York, 1987).
8. B. PREDEL, L. RATKE and H. FREDRIKSSON, in "Fluid Science and Materials Science in Space," edited by H.U. Walter (Springer-Verlag, New York, 1987).
9. L. VAN VUGT and L. FROYEN, *Microgravity Sci. Technol.* **X(2)** (1997) 95.
10. T. IIDA and R. I. L. CUTHRIE, "The Physical Properties of Liquid Metals" (Clarendon Press, Oxford, 1993).
11. E. O. KIRKENDALL, *Trans. Amer. Inst. Mining Met. Eng.* **147** (1942) 104.
12. A. D. SMIGELSKAS and E. O. KIRKENDALL, *ibid.* **171** (1947) 130.
13. L. S. DARKEN, *ibid.* **175** (1948) 184.
14. J. R. MANNING, *Phys. Rev.* **124**(2) (1961) 470.
15. D. B. BUTRYMOWICZ and J. R. MANNING, *Met. Trans.* **9A** (1978) 947.
16. M. J. DALLWITZ, *Acta. Met.* **20** (1972) 1229.
17. J. L. BOCQUET, G. BREBEC and Y. LIMOGE, in "Physical Metallurgy," edited by R. W. Cahn and P. Haasen (North-Holland Physics Publ., Amsterdam, 1983) ch. 7, section 5.
18. A. A. ZJUHOVITSKIJ and L. L. SCHWARZMAN, in "Physical Chemistry" (Moscow, Metallurgija Publ., 1976) (in russian).
19. M. ONISHI, C. G. LEE, J. H. YOON and T. SHIMOZAKI, *J. Japan Inst. Metals* **62** (1998) 505.
20. F. J. J. VAN LOO, B. PIERAGGI and R. A. RAPP, *Acta Met. and Mater.* **38** (1990) 1769.
21. K. NORDLUND and R. S. AVERBACK, *Phys. Review* B **59** (1999) 20.
22. J. S. KIRKALDY and G. SAVVA, *Acta Mater.* **45** (1997) 3115.
23. Z. RADI, P. B. BARNA and J. LABAR, *J. Appl. Phys.* **79** (1996) 4096.